In Vivo Formation and in Vitro Replication of a Guanine−Thymine Intrastrand Cross-Link Lesion†

Yong Jiang,‡ Haizheng Hong,‡ Huachuan Cao,§ and Yinsheng Wang*,‡,§

Environmental Toxicology Graduate Program and Department of Chemistry, University of California at Riverside, Riverside, California 92521

Received June 20, 2007; Revised Manuscript Received August 26, 2007

ABSTRACT: G[8−5m]T, a guanine−thymine intrastrand cross-link lesion where the C8 of guanine is covalently bonded to the neighboring 3′-thymine through its methyl carbon, was previously shown to form in an aqueous solution of duplex DNA upon exposure to γ- or X-rays and in calf thymus DNA treated with Fenton reagents. Here, we employed LC−MS/MS and demonstrated for the first time that this lesion could be induced in a dose-dependent manner in human Hela-S3 cells upon exposure to γ-rays. We further carried out in vitro replication studies on a substrate containing a site-specifically incorporated G[8−5m]T, and our results showed that the Klenow fragment of *Escherichia coli* DNA polymerase I stopped synthesis mostly after incorporating the correct nucleotide dAMP opposite the 3′-thymine moiety of the lesion. On the other hand, yeast *Saccharomyces cerevisiae* DNA polymerase η (pol η) was able to replicate past the cross-link lesion, but with markedly reduced efficiency in nucleotide incorporation opposite the 5′-guanine of the lesion. Steady-state kinetic analyses for nucleotide incorporation by yeast pol η showed that the 5′-guanine portion of the lesion also decreased pronouncedly the fidelity of nucleotide incorporation; the insertion of dAMP and dGMP was favored over that of the correct nucleotide, dCMP. The above results support the conclusion that oxidative intrastrand cross-link lesions, if not repaired, can be cytotoxic and mutagenic.

Excess generation of reactive oxygen species (ROS)[1] in vivo can result in DNA damage (*1*−*3*), which includes a multitude of single-nucleobase lesions (*4*) and a number of intrastrand cross-link lesions (*5*−*17*). In this respect, Bellon et al. (*10*) found that some intrastrand cross-link lesions, including G[8−5m]T, where the C8 of guanine is covalently bonded to the methyl carbon of its neighboring 3′-thymine (structure shown in Figure 1), can be induced in an aqueous solution of duplex DNA upon exposure to γ-rays. In addition, our recent study demonstrated that G[8−5m]T could be generated from calf thymus DNA upon treatment with Fenton reagent, Cu(II)/H_2O_2/ascorbate, under aerobic conditions (*18*).

Previous studies revealed that intrastrand cross-link lesions are initiated from a single pyrimidine radical (*6*−*8, 10, 12*−*14*). In this respect, the hydroxyl radical (•OH) can abstract a hydrogen atom from the 5-methyl group of thymine (*19*), leading to the formation of the methyl radical of the nucleobase, which may attack its neighboring guanine base to yield G[8−5m]T (*10*). In light of this underlying mechanism for the formation of the intrastrand cross-link lesions and the previous results from the treatment of calf thymus DNA with Fenton-type reagents (*18*), we reasoned that the G[8−5m]T cross-link lesion might be induced in genomic DNA of eukaryotic cells upon exposure to ROS.

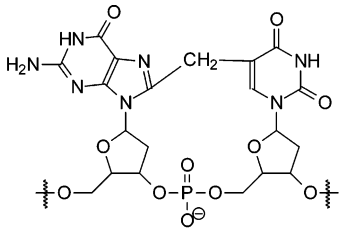

FIGURE 1: (Top) Structure of the G[8−5m]T intrastrand cross-link. (Bottom) Substrates used for in vitro replication studies. The sequence was chosen because the corresponding in vitro replication study for the structurely related G[8−5]C intrastrand cross-link was carried out with the lesion situated in the same sequence context (*17*, *29*).

Cells have developed various strategies to minimize the deleterious effects of DNA lesions by an intricate DNA repair system and certain mechanisms to tolerate unrepaired or highly repair-resistant DNA lesions during DNA replication (*20*, *21*). However, the presence of DNA lesions in replicating DNA may lead to the stalling of DNA replication, which

† This work was supported by the National Institutes of Health (Grants R01 CA96906 and R01 CA101864).

* To whom correspondence should be addressed. Phone: (951) 827-2700. Fax: (951) 827-4713. E-mail: yinsheng.wang@ucr.edu.

‡ Environmental Toxicology Graduate Program.

§ Department of Chemistry.

[1] Abbreviations: ROS, Reactive oxygen species; pol η, polymerase η; NER, nucleotide excision repair; XP-V, variant form of xeroderma pigmentosum; ODN, oligodeoxyribonucleotide; TLC, translesion synthesis; SIC, selected-ion chromatogram; thymidine glycol, 5,6-dihydroxy-5,6-dihydrothymidine; 8-oxodG, 8-oxo-7,8-dihydro-2′-deoxyguanosine.

10.1021/bi7012195 CCC: $37.00
Published on Web 10/12/2007

may cause cell death. Moreover, lesions may give rise to mutations and result in numerous pathological conditions including cancer and aging (*20*). Other than some frequently observed single-base substitutions emanating from ROS-induced DNA lesions, e.g., C → T transitions and G → T transversions (*22*), CC → TT and mCG → TT tandem double mutations were shown to be induced by ROS generated from a variety of systems (*22*−*25*). It has been suggested that ROS-induced intrastrand cross-link lesions formed between adjacent nucleotides might contribute to the tandem mutations (*23*, *24*). In addition, both G[8−5]C and G[8−5m]T cross-link lesions could be substrates for the nucleotide excision repair (NER) pathway (*26*, *27*).

It was proposed that, when a high-fidelity replication fork is arrested at the sites of DNA damage, translesion synthesis (TLS) polymerases can take over from replicative polymerases temporarily to bypass synthetically the templates with lesions. This process can be either error-free or error-prone (*28*). Our previous in vitro replication studies on G[8−5]C showed that it can either stall DNA replication performed by some high-fidelity replicative polymerases, such as T7 DNA polymerase and HIV reverse transcriptase, or lead to mutagenesis by a translesion synthesis polymerase, yeast polymerase η (*17*, *29*).

In this study, we demonstrated, for the first time, that the G[8−5m]T cross-link lesion could be induced, in a dose-dependent manner, in cultured human cells upon exposure to γ-rays. In addition, we measured the steady-state kinetic parameters during DNA replication in vitro with a replicative DNA polymerase, the Klenow fragment (KF) of *Escherichia coli* DNA polymerase I, and a member of the "Y" superfamily of polymerases, yeast DNA polymerase η. The latter is the gene product of Rad30 in budding yeast *Saccharomyces cerevisiae* (*30*) and the variant form of xeroderma pigmentosum (XP-V) in humans (*31*).

MATERIALS AND METHODS

Chemicals and Enzymes. All unmodified oligodeoxyribonucleotides (ODNs) used in this study were purchased from Integrated DNA Technologies (Coralville, IA). [γ-^{32}P]ATP was obtained from Amersham Biosciences Co. (Piscataway, NJ). Other chemicals were purchased from Sigma-Aldrich (St. Louis, MO). Nuclease P1 and alkaline phosphatase were procured from MP Biomedicals (Aurora, OH) and Sigma-Aldrich (St. Louis, MO), respectively. Snake venom phosphodiesterase and calf spleen phosphodiesterase were obtained from US Biological (Swampscott, MA). The Klenow fragment (3′ → 5′ exo$^-$) of *E. coli* DNA polymerase I was purchased from New England Biolabs, Inc. (Ipswich, MA). Yeast polymerase η (pol η) was expressed and purified following previously published procedures (*32*). Hela-S3 cells were obtained from the National Cell Culture Center (Minneapolis, MN).

Treatment of Hela-S3 Cells with γ-Rays and Enzymatic Digestion of DNA. Hela-S3 cells were centrifuged to remove the culture medium and resuspended in phosphate-buffered saline. The cell suspension (10^7 cells/mL) was exposed to γ-rays delivered by a Mark I ^{137}Cs irradiator (JL Shepherd and Associates, San Fernando, CA). The dose rate was maintained at 2.8 Gy/min, and irradiation was continued until a certain total dose of exposure was reached. Immediately after the exposure, the cells were harvested by centrifugation and the nuclear DNA was isolated by phenol extraction following previously published procedures (*33*).

The DNA was digested with four enzymes (nuclease P1, calf spleen phosphodiesterase, alkaline phosphatase, and snake venom phosphodiesterase) to release the intrastrand cross-link lesions as dinucleoside monophosphates following previously described procedures (*34*). The digestion mixture was passed through a YM-10 Centricon membrane (Millipore, Billerica, MA) to remove the enzymes. The amount of nucleosides in the mixture was quantified by UV absorption spectroscopy. To the mixture was then added isotopically labeled d(G[8−5m]T) (*18*), which carried two ^{15}N atoms and a deuterium on the thymidine portion.

HPLC Enrichment. The HPLC enrichment of d(G[8−5m]T) from the digestion mixture of cellular DNA was performed with a 4.6 × 50 mm Luna reversed-phase C18 column (5 μm in particle size, Phenomenex, Torrance, CA). A gradient of 5 min of 0−2% acetonitrile followed by 55 min of 2−5% acetonitrile in 10 mM ammonium formate (pH 6.3) was employed, and the flow rate was 0.60 mL/min. The fractions were collected in a wide retention time range to ensure that the cross-link product was completely collected. The collected fractions were dried in the SpeedVac, redissolved in 15 μL of H_2O, and injected for LC−MS/MS analysis.

LC−MS/MS for the Detection and Quantification of G[8−5m]T. A 0.5 × 150 mm Zorbax SB-C18 column (particle size 5 μm, Agilent Technologies, Palo Alto, CA) was used for the separation of the DNA hydrolysis samples, and the flow rate was 8.0 μL/min, which was delivered by an Agilent 1100 capillary HPLC pump (Agilent Technologies). A 60 min gradient of 0−30% acetonitrile in 20 mM ammonium acetate was employed for the analysis of HPLC-enriched d(G[8−5m]T). The effluent from the LC column was coupled to an LTQ linear ion-trap mass spectrometer (Thermo Fisher Scientific, San Jose, CA), which was set up for monitoring the fragmentation of the $[M + H]^+$ ions of the labeled and unlabeled d(G[8−5m]T).

Preparation of Substrates for in Vitro Replication Studies. The G[8−5m]T-containing ODN for in vitro replication studies was prepared following procedures described in a previous paper (*26*). Briefly, a dodecameric lesion-bearing substrate, d(ATGGCG[8−5m]TGCTAT), was obtained from the 254 nm irradiation of a 5-[(phenylthio)methyl]-2′-deoxyuridine-containing ODN. The lesion-bearing substrate was ligated with the 5′-phosphorylated d(GATCCTAG) in the presence of a template ODN, d(CCGCTCCCTAGGATCATAGCACGCCAT) (*17*). The desired lesion-containing 20-mer ODN was purified by using 20% denaturing polyacrylamide gel electrophoresis (PAGE) and desalted by ethanol precipitation. The purity of the product was further confirmed by PAGE analysis.

Primer Extension Assay. The 20-mer lesion-containing template or the normal template (20 nM) with GT in lieu of G[8−5m]T was annealed with a 5′-^{32}P-labeled 14-mer primer (10 nM). To the duplex mixture were added a mixture of all four dNTPs and a DNA polymerase. The reaction was carried out at 37 °C in a buffer containing 10 mM Tris−HCl (pH 7.5), 5 mM $MgCl_2$, and 7.5 mM DTT for 60 min. The concentrations of the polymerases are indicated in the figures. The reaction was terminated by adding a 2 volume excess

of formamide gel-loading buffer [80% formamide, 10 mM EDTA (pH 8.0), 1 mg/mL xylene cyanol, and 1 mg/mL bromophenol blue]. The products were resolved on 20% (29:1) cross-linked polyacrylamide gels containing 8 M urea. Gel band intensities for the substrates and products were quantified by using a Typhoon 9410 variable-mode imager (Amersham Biosciences Co.) and ImageQuant version 5.2 (Amersham Biosciences Co.).

Steady-State Kinetic Measurements. The steady-state kinetic analyses were performed as described previously (*35*, *36*). In this measurement, the primer−template duplex (10 nM) was incubated with either Klenow fragment (0.1 unit) or yeast polymerase η (5 ng) in the presence of an individual dNTP at various concentrations as indicated in the figures. The reaction was carried out at room temperature with the same reaction buffer as described for the primer extension assays. The dNTP concentration was optimized for different insertion reactions to allow for less than 20% primer extension (*36*). The observed rate of dNTP incorporation (V_{obsd}) was plotted as a function of dNTP concentration, and the apparent K_m and V_{max} steady-state kinetic parameters for the incorporation of both the correct and incorrect nucleotides were determined by fitting the rate data with the Michaelis−Menten equation:

$$V_{obsd} = \frac{V_{max}[\text{dNTP}]}{K_m + [\text{dNTP}]}$$

The efficiency of nucleotide incorporation was determined by the ratio V_{max}/K_m. The fidelity of nucleotide incorporation was then calculated by the frequency of misincorporation (f_{inc}) with the following equation:

$$f_{inc} = \frac{(V_{max}/K_m)_{incorrect}}{(V_{max}/K_m)_{correct}}$$

Molecular Modeling. Molecular modeling was carried out on a Silicon Graphics O2 workstation (SGI, Sunnyvale, CA) with Spartan (SGI version 5.1.3, Wavefunction, Inc., Irvine, CA). The initial geometry of d(G[8−5m]T) was built from d(GT) by employing standard B-DNA parameters and optimized with the semiempirical PM3 method (*37*).

RESULTS

Identification and Quantification of G[8−5m]T in Hela-S3 Cells Exposed to γ-Rays. Encouraged by the findings that G[8−5m]T could be induced in ODNs from exposure to γ-rays and in calf thymus DNA treated with Fenton reagents under aerobic conditions (*10*, *18*), we set out to examine the formation of this type of lesion in human cells. To this end, we exposed cultured Hela-S3 cells to a series of doses of γ-rays, isolated the nuclear DNA immediately after the exposure, and digested the DNA by using four enzymes (see the Materials and Methods). This digestion method was proven to be efficient in liberating both single-nucleobase and intrastrand cross-link lesions (*18*). We then added the isotope-labeled d(G[8−5m]T) to the digestion mixture, removed most unmodified nucleosides by HPLC, and subjected the d(G[8−5m]T)-containing HPLC fractions to LC−MS/MS and LC−MS/MS/MS (MS^3) analyses.

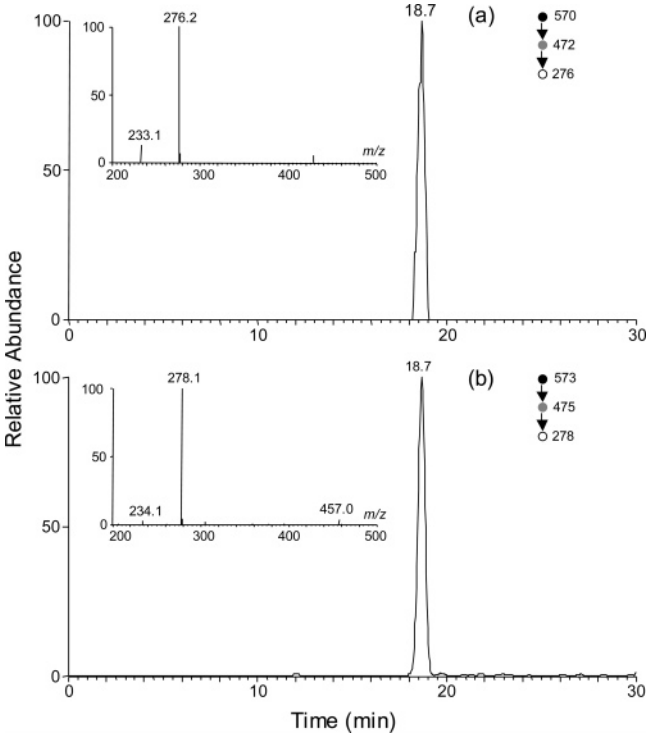

FIGURE 2: SICs for monitoring the *m*/*z* 570 → 472 → 276 (a, for unlabeled d(G[8−5m]T)) and *m*/*z* 573 → 475 → 278 (b, for labeled d(G[8−5m]T)) transitions in the γ-ray-treated DNA after enzymatic digestion. Shown in the insets are the MS^3 results for the unlabeled and labeled d(G[8−5m]T).

Our LC−MS results revealed that G[8−5m]T could be induced in cultured human cells upon exposure to γ-rays. In this context, we observed a peak in the selected-ion chromatogram (SIC) for the *m*/*z* 570 → 472 transition for the DNA sample obtained from the cells (Figure S1 in the Supporting Information). Moreover, the product-ion spectrum of the $[M + H]^+$ ion of this fraction showed the presence of the fragment ion of *m*/*z* 472 (Figure S1), which is attributed to the elimination of a 2-deoxyribose (*18*). Corresponding analysis of DNA samples obtained from control cells without γ-ray exposure revealed that G[8−5m]T was not detectable. In this respect, we chose to employ positive-ion ESI-MS for assessing the formation of G[8−5m]T because the sensitivity for analyzing this compound is greater in the positive-ion mode than in the negative-ion mode.

Other than the characteristic fragment ion found in the MS/MS spectrum for the internal standard and the analyte, ions from impurities were also present (Figure S1). To afford unambiguous detection of the lesion, we set up the instrument to monitor the further cleavage of the ion of *m*/*z* 472 to obtain a product-ion spectrum, i.e., MS^3, of high quality (Figure 2). In this respect, collisional activation of the ion of *m*/*z* 472 results in the formation of a dominant fragment ion of *m*/*z* 276, which is attributed to the protonated species of the cross-linked nucleobase component. Moreover, the LC−MS^3 results revealed the dose-dependent formation of this lesion in Hela-S3 cells (Figure 3, and the calibration curve is shown in Figure S2 of the Supporting Information). It is worth noting that the rate for the formation of the G[8−5m]T lesion is approximately 0.050 (lesion/10^9 nucleosides)/Gy, which is approximately 200 times lower than what we recently found for the rate of the formation of 5-formyl-2′-deoxyuri-

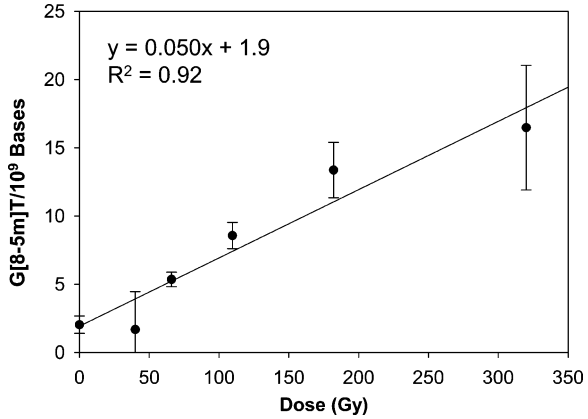

FIGURE 3: Dose-dependent formation of G[8−5m]T in Hela-S3 cells upon exposure to γ-rays. The values represent the means ± SD from three independent exposure and quantification experiments.

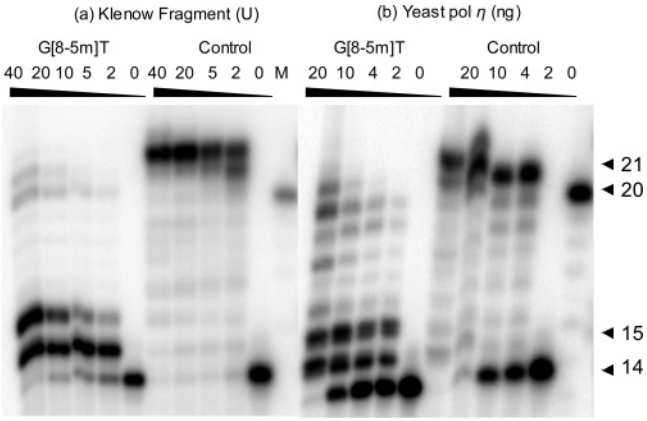

FIGURE 4: Primer extension assays for nucleotide incorporation opposite a G[8−5m]T-bearing substrate and its control undamaged substrate with exo$^-$ Klenow fragment (left two panels) and yeast pol η (right two panels). The sequences for the control and G[8−5]T-bearing templates are listed in Figure 1, and 5′-[^{32}P]-labeled d(GCTAGGATCATAGC) was used as the primer. KF (exo$^-$) or yeast pol η with the indicated concentrations was incubated with 10 nM substrate and 200 μM dNTPs at 37 °C for 60 min.

dine (0.011 (lesion/10^6 nucleotides)/Gy) under identical exposure conditions (*33*).

In Vitro Replication Studies of the G[8−5m]T Cross-Link Lesion. The G[8−5m]T-bearing 12-mer ODN substrate was obtained from the 254 nm irradiation of a 5-[(phenylthio)-methyl]-2′-deoxyuridine-containing ODN following previously reported procedures (*26*). This lesion-carrying ODN was further ligated with a 5′-phosphorylated 8-mer ODN to construct a 20-mer lesion-containing substrate as a template for in vitro replication studies (Figure 1).

First, we performed primer extension assays on the G[8−5m]T-bearing substrate with Klenow fragment and yeast pol η. The results with the Klenow fragment showed that, in the presence of all four dNTPs, the synthesis stopped mostly after the incorporation of the first nucleotide opposite the 3′-T of the lesion. A small portion of the reaction product carried an additional nucleotide opposite the 5′-G of the lesion, and only a trace amount of full-length products could be detected (Figure 4a). This result is consistent with what was recently observed by Bellon and co-workers (*38*). On the other hand, the primer extension assay with yeast pol η showed that this polymerase can partially bypass the G[8−5 m]T intrastrand cross-link when all four dNTPs are present.

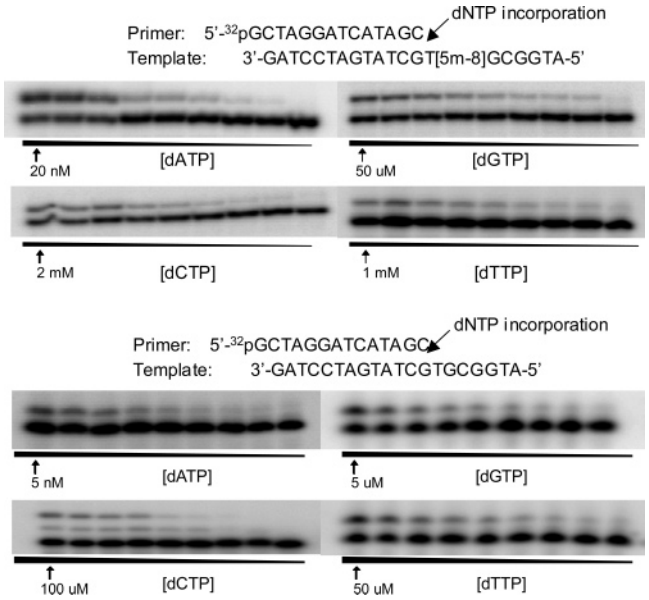

FIGURE 5: Steady-state kinetic measurements for the incorporation of dAMP, dGMP, dCMP, and dTMP opposite the thymidine portion of G[8−5m]T (top panels) or opposite the thymidine at an undamaged GT site (bottom panels). Exo$^-$ Klenow fragment (0.1 U) was incubated with 10 nM DNA substrate at room temperature for 10 min. The highest dNTP concentration is shown in the figure, and the concentration ratio of dNTP between adjacent lanes was 0.5−0.6.

However, a considerable number of short replication products with the addition of one or two nucleotides opposite the lesion site were also found (Figure 4b).

Next, we determined the steady-state kinetic parameters for nucleotide incorporation opposite the damaged nucleobases in the G[8−5m]T lesion-containing substrate and G and T in the undamaged substrate as a control by both Klenow fragment and yeast pol η (Figure 5 and Figure S3 in the Supporting Information). The steady-state kinetic parameters for nucleotide incorporation mediated by the two polymerases are summarized in Tables 1 and 2.

Relative to that for the unmodified substrate, the efficiency for Klenow fragment to incorporate the correct nucleotide, dAMP, opposite the 3′-thymine moiety of G[8−5m]T was reduced by only 2-fold. Decreased incorporation efficiencies, i.e., by 2−10 times, were also found for the other three nucleotides. Thus, the incorporation of dAMP is still much more preferred over those of the other three nucleotides in the presence of the lesion (Table 1). However, when we attempted to measure the steady-state kinetic parameters for nucleotide incorporation opposite the 5′-guanine moiety of the lesion with the Klenow fragment, we either could not detect any nucleotide incorporation or failed to derive valid kinetic parameters within the applicable concentration range (<2 mM) of dNTPs. The results indicate that, although one nucleotide can be incorporated opposite the 3′-T moiety, DNA synthesis is blocked mostly at the 5′-G moiety of the G[8−5m]T lesion. This result is consistent with results obtained from the primer extension assay (vide supra).

We further measured the steady-state kinetic parameters for nucleotide incorporation catalyzed by yeast pol η. When the data for the lesion-containing and undamaged substrates were compared, we found that the presence of the cross-link lesion diminished the insertion efficiencies of all four

Table 1: Fidelity of Nucleotide Incorporation by Exo$^-$ Klenow Fragment on a G[8−5m]T Cross-Link-Containing Substrate and the Undamaged Substrate As Determined by Steady-State Kinetic Measurements[a]

dNTP	V_{max} (nM/min)	K_m (nM)	V_{max}/K_m	f_{inc}
G[8−5m]T-Containing Substrate (14-mer Primer, 5′-GCTAGGATCATAGC-3′)				
dATP	0.22 ± 0.004	0.71 ± 0.02	0.31	1.0
dGTP	0.29 ± 0.02	(6 ± 1) × 10^2	5 × 10^{-4}	2 × 10^{-3}
dCTP	0.28 ± 0.01	(4.0 ± 0.4) × 10^4	7.0 × 10^{-6}	2.3 × 10^{-5}
dTTP	0.24 ± 0.004	(1.07 ± 0.05) × 10^5	2.2 × 10^{-5}	7.1 × 10^{-5}
Undamaged DNA Substrate (14-mer Primer, 5′-GCTAGGATCATAGC-3′)				
dATP	0.27 ± 0.01	1.63 ± 1.60	0.16	1.0
dGTP	0.17 ± 0.04	(4 ± 1) × 10^3	4 × 10^{-5}	2 × 10^{-4}
dCTP	0.16 ± 0.01	(5.2 ± 0.5) × 10^4	3.1 × 10^{-6}	1.9 × 10^{-5}
dTTP	0.10 ± 0.001	(3.0 ± 0.3) × 10^4	3.3 × 10^{-6}	2.0 × 10^{-5}

[a] K_m and V_{max} are average values based on three independent measurements.

Table 2: Fidelity of Nucleotide Incorporation by Yeast Polymerase η on a G[8−5m]T Cross-Link-Containing Substrate and the Undamaged Substrate As Determined by Steady-State Kinetic Measurements[a]

dNTP	V_{max} (nM/min)	K_m (nM)	V_{max}/K_m	f_{inc}
G[8−5m]T-Containing Substrate, 14-mer Primer (5′-GCTAGGATCATAGC-3′)				
dATP	0.40 ± 0.02	(3.3 ± 0.5) × 10^2	1.2 × 10^{-3}	1.0
dGTP	0.45 ± 0.06	(1.7 ± 0.3) × 10^5	2.7 × 10^{-6}	2.3 × 10^{-3}
dCTP	0.20 ± 0.01	(8 ± 2) × 10^3	3 × 10^{-5}	2 × 10^{-2}
dTTP	0.38 ± 0.07	(1.2 ± 0.4) × 10^5	3.1 × 10^{-6}	2.6 × 10^{-3}
Undamaged Substrates, 14-mer Primer (5′-GCTAGGATCATAGC-3′)				
dATP	0.23 ± 0.02	36.1 ± 0.6	6.4 × 10^{-3}	1.0
dGTP	0.33 ± 0.02	(5.9 ± 0.5) × 10^4	5.6 × 10^{-6}	8.8 × 10^{-4}
dCTP	0.32 ± 0.04	(4.1 ± 0.1) × 10^3	7.8 × 10^{-5}	1.2 × 10^{-2}
dTTP	0.53 ± 0.01	(1.1 ± 0.9) × 10^5	4.6 × 10^{-6}	7.2 × 10^{-4}
G[8−5m]T-Containing Substrate, 15-mer Primer (5′-GCTAGGATCATAGCA-3′)				
dATP	0.48 ± 0.03	(5.0 ± 0.6) × 10^4	9.5 × 10^{-6}	1.0
dGTP	0.32 ± 0.01	(5.7 ± 0.2) × 10^4	5.6 × 10^{-6}	0.59
dCTP	0.47 ± 0.05	(2.3 ± 0.2) × 10^6	2.1 × 10^{-7}	2.2 × 10^{-2}
dTTP	0.33 ± 0.02	(6.2 ± 0.4) × 10^5	5.3 × 10^{-7}	5.6 × 10^{-2}
Undamaged Substrate, 15-mer Primer (5′-GCTAGGATCATAGCA-3′)				
dATP	0.97 ± 0.08	(5.2 ± 0.3) × 10^5	1.9 × 10^{-6}	4.8 × 10^{-5}
dGTP	1.57 ± 0.01	(5.77 ± 0.07) × 10^5	2.7 × 10^{-6}	7.0 × 10^{-5}
dCTP	0.36 ± 0.04	9.2 ± 2.5	3.9 × 10^{-2}	1.0
dTTP	0.36 ± 0.04	(1.8 ± 0.3) × 10^4	2.0 × 10^{-5}	5.1 × 10^{-4}

[a] K_m and V_{max} are average values based on three independent measurements.

dNTPs opposite the 3′-T moiety of the lesion by nearly 1−5 times (Table 2). As a result, pol η still inserted dAMP opposite the 3′-T of the lesion most preferentially. The incorporation efficiency of the correct nucleotide, dCMP, opposite the 5′-G, however, is markedly reduced, i.e., by approximately 5 orders of magnitude, with the presence of the cross-link lesion (a 15-mer primer with a dA at the 3′-terminus was used for this measurement, Table 2). On the other hand, the efficiencies for the insertion of dAMP and dGMP opposite the 5′-G of the lesion became slightly higher than those for the incorporation of these two nucleotides opposite an unmodified guanine. Consequently, the fidelity of nucleotide incorporation opposite the 5′-G moiety of the lesion was significantly impaired. The insertion of dAMP or dGMP was slightly favored over that of dCMP or dTMP. This result indicates that, during translesion synthesis by yeast pol η, the existence of the G[8−5m]T intrastrand cross-link lesion in the template may lead to the incorporation of a dAMP or dGMP opposite the 5′-G moiety instead of the correct dCMP, thereby giving rise to G → T and G → C transversions.

It is worth emphasizing that, even though yeast pol η can synthetically bypass both nucleobases of the cross-link lesion, in addition to the compromised fidelity, the efficiency for nucleotide incorporation opposite the 5′-G dropped by approximately 4000 times. Therefore, the presence of the G[8−5m]T cross-link lesion decreases both the efficiency and the fidelity of nucleotide incorporation mediated by yeast pol η. In this context, it is of note that, the efficiency for nucleotide incorporation by yeast pol η opposite an abasic site was also reduced significantly, i.e., by 3 orders of magnitude, in relation to the nucleotide insertion opposite an undamaged site (*39*). On the other hand, yeast pol η inserts the correct nucleotide opposite the 5,6-dihydroxy-5,6-dihydrothymidine (thymidine glycol) and 8-oxo-7,8-dihydro-2′-deoxyguanosine (8-oxodG), which are commonly observed oxidative single-nucleobase lesions formed at thymidine and 2′-deoxyguanosine sites, respectively (*40*, *41*). In addition, the nucleotide insertion opposite these two lesions is as efficient as the corresponding nucleotide incorporation opposite the undamaged counterparts (*40*, *41*).

DISCUSSION

By using LC−MS/MS with the standard isotope dilution method, we demonstrated, for the first time, that G[8−5m]T could be induced in Hela-S3 cells upon exposure to γ-rays. This result, combined with our previous finding that the lesion could be generated in calf thymus DNA upon

treatment with Fenton reagents under aerobic conditions (*18*), underlies the biological significance of this type of lesion.

As reported previously, a photochemical approach enabled us to obtain well-characterized intrastrand cross-link-containing ODNs (*26*). In this context, ODN substrates bearing a structurally defined lesion for in vitro replication studies facilitate us to understand the biological implications of these lesions at the molecular level. Examining the behaviors of both a replicative polymerase and a translesion synthesis polymerase during DNA replication provides us with a comprehensive view of the mutagenic properties of a DNA lesion. Our results revealed that both Klenow fragment and yeast pol η could incorporate the correct nucleotide, dAMP, opposite the 3′-T of the lesion with a relatively high efficiency. Thus, the hydrogen-bonding properties of the 3′-T might be conferred during nucleotide incorporation by both polymerases, though Klenow fragment belongs to the high-fidelity "A" family of DNA polymerases, which adopt constrained active sites (*42*, *43*). On the other hand, the efficiency for nucleotide incorporation by Klenow fragment opposite the 5′-G was diminished markedly by the presence of the G[8−5m]T lesion. In addition, the 5′-G portion of the cross-link lesion conferred a significant drop in efficiencies for nucleotide incorporation by yeast pol η. Moreover, yeast pol η-mediated nucleotide insertion opposite the 5′-G was error-prone, with dGMP and dAMP being incorporated much more efficiently than the correct nucleotide, dCMP.

We reason that the presence of the cross-link lesion may lead to a structural distortion to duplex DNA, which may render the hydrogen-bonding property of the 5′-guanine portion not to be recognized by yeast pol η during nucleotide insertion. Indeed, molecular modeling results with the semiempirical PM3 method (*37*) predicted that the *N*-glycosidic linkage of the 3′-nucleoside of the cross-link assumes an *anti* configuration, whereas that of the 5′-nucleoside is closer to a *syn* than an *anti* configuration (Figure S4; coordinates for the optimized structure can be found in the PDB file in the Supporting Information). Under such circumstances, purine nucleotides can conceivably be incorporated opposite the 5′-G more efficiently than pyrimidine nucleotides because the former nucleotides exhibit a stronger stacking interaction with the 3′-nucleotide of the primer than the latter nucleotides (*44*). In this context, it is worth noting that the efficiencies and specificities of nucleotide incorporation opposite G[8−5m]T by yeast pol η are consistent with our previous observations with the G[8−5]C lesion (*17*).

The significant structure distortion as predicted by molecular modeling is consistent with the destabilizing effect of the lesion on duplex DNA. Indeed thermodynamic parameters derived from melting temperature measurements revealed that G[8−5m]T destabilized the duplex, due to an increase in free energy for duplex formation at 37 °C, by approximately 3.6 kcal/mol (*26*). In addition, the PM3-optimized structure underscores that the structure distortion of the 2′-deoxyguanosine portion of the intrastrand cross-link is expected to perturb the stacking of this modified guanine component with its neighboring unmodified 5′-nucleobase.

G[8−5m]T could be recognized by the *E. coli* UvrABC nuclease, suggesting that this lesion may be a good substrate for the NER pathway in vivo (*26*, *27*). Therefore, the presence of the lesion is expected to have significant biological consequences, especially for people suffering from genetic diseases associated with deficiency in NER, i.e., xeroderma pigmentosum (XP) (*45*). XP patients often exhibit a progressive, yet massive, neuron loss, which is accompanied by mental deterioration (*46*). The accumulation of oxidative intrastrand cross-link lesions may contribute to the pathophysiological symptoms of the XP patients.

The intracellular concentrations of iron and copper ions can be dramatically elevated under oxidative stress conditions via the release of these ions from iron- or copper-storage proteins (*47*, *48*). In humans, genetic hemochromatosis and Wilson's disease induce abnormal accumulation of iron and copper, respectively, in various organs. Bulky DNA lesions were found in the liver of patients with Wilson's disease and primary hemochromatosis (*49*). On the grounds that oxidative intrastrand cross-link lesions could be induced in DNA by iron- or copper-mediated Fenton-type reactions (*18*, *50*), we reason that this type of lesion may also play a role in the pathological conditions associated with high intracellular concentrations of these transition-metal ions.

ACKNOWLEDGMENT

We thank Prof. John-Stephen A. Taylor at Washington University for providing the construct for the overexpression of yeast pol η.

SUPPORTING INFORMATION AVAILABLE

LC−MS/MS data, primer extension assay results, and PDB file for the PM3-optimized structure of d(G[8−5m]T). This material is available free of charge via the Internet at http://pubs.acs.org.

REFERENCES

1. Lindahl, T. (1999) DNA lesions generated in vivo by reactive oxygen species, their accumulation and repair, *NATO ASI Ser., Ser. A 302*, 251−257.
2. Finkel, T., and Holbrook, N. J. (2000) Oxidants, oxidative stress and the biology of ageing, *Nature 408*, 239−247.
3. Marnett, L. J. (2000) Oxyradicals and DNA damage, *Carcinogenesis 21*, 361−370.
4. Dizdaroglu, M., Jaruga, P., Birincioglu, M., and Rodriguez, H. (2002) Free radical-induced damage to DNA: mechanisms and measurement, *Free Radical Biol. Med. 32*, 1102−1115.
5. Box, H. C., Budzinski, E. E., Dawidzik, J. D., Wallace, J. C., Evans, M. S., and Gobey, J. S. (1996) Radiation-induced formation of a crosslink between base moieties of deoxyguanosine and thymidine in deoxygenated solutions of d(CpGpTpA), *Radiat. Res. 145*, 641−643.
6. Box, H. C., Budzinski, E. E., Dawidzik, J. B., Gobey, J. S., and Freund, H. G. (1997) Free radical-induced tandem base damage in DNA oligomers, *Free Radical Biol. Med. 23*, 1021−1030.
7. Box, H. C., Budzinski, E. E., Dawidzik, J. B., Wallace, J. C., and Iijima, H. (1998) Tandem lesions and other products in X-irradiated DNA oligomers, *Radiat. Res. 149*, 433−439.
8. Budzinski, E. E., Dawidzik, J. B., Rajecki, M. J., Wallace, J. C., Schroder, E. A., and Box, H. C. (1997) Isolation and characterization of the products of anoxic irradiation of d(CpGpTpA), *Int. J. Radiat. Biol. 71*, 327−336.
9. Romieu, A., Bellon, S., Gasparutto, D., and Cadet, J. (2000) Synthesis and UV photolysis of oligodeoxynucleotides that contain 5- (phenylthiomethyl)-2′-deoxyuridine: a specific photolabile precursor of 5-(2′-deoxyuridilyl)methyl radical, *Org. Lett. 2*, 1085−1088.
10. Bellon, S., Ravanat, J. L., Gasparutto, D., and Cadet, J. (2002) Cross-linked thymine-purine base tandem lesions: synthesis, characterization, and measurement in gamma-irradiated isolated DNA, *Chem. Res. Toxicol. 15*, 598−606.

11. Zeng, Y., and Wang, Y. (2004) Facile formation of an intrastrand cross-link lesion between cytosine and guanine upon pyrex-filtered UV light irradiation of d((Br)CG) and duplex DNA containing 5-bromocytosine, *J. Am. Chem. Soc. 126*, 6552−6553.
12. Zhang, Q., and Wang, Y. (2003) Independent generation of 5-(2′-deoxycytidinyl)methyl radical and the formation of a novel crosslink lesion between 5-methylcytosine and guanine, *J. Am. Chem. Soc. 125*, 12795−12802.
13. Zhang, Q., and Wang, Y. (2004) Independent generation of the 5-hydroxy-5,6-dihydrothymidin-6-yl radical and its reactivity in dinucleoside monophosphates, *J. Am. Chem. Soc. 126*, 13287−13297.
14. Zhang, Q., and Wang, Y. (2005) Generation of 5-(2′-deoxycytidyl)-methyl radical and the formation of intrastrand cross-link lesions in oligodeoxyribonucleotides, *Nucleic Acids Res. 33*, 1593−1603.
15. Liu, Z., Gao, Y., and Wang, Y. (2003) Identification and characterization of a novel crosslink lesion in d(CpC) upon 365 nm-irradiation in the presence of 2-methyl-1,4-naphthoquinone, *Nucleic Acids Res. 31*, 5413−5424.
16. Liu, Z., Gao, Y., Zeng, Y., Fang, F., Chi, D., and Wang, Y. (2004) Isolation and characterization of a novel cross-link lesion in d(CpC) induced by one-electron photooxidation, *Photochem. Photobiol. 80*, 209−215.
17. Gu, C., and Wang, Y. (2004) LC-MS/MS identification and yeast polymerase eta bypass of a novel gamma-irradiation-induced intrastrand cross-link lesion G[8−5]C, *Biochemistry 43*, 6745−6750.
18. Hong, H., Cao, H., Wang, Y., and Wang, Y. (2006) Identification and quantification of a guanine-thymine intrastrand cross-link lesion induced by Cu(II)/H_2O_2/ascorbate, *Chem. Res. Toxicol. 19*, 614−621.
19. von Sonntag, C. (1987) *The Chemical Basis of Radiation Biology*, Taylor & Francis, London.
20. Friedberg, E. C., Walker, G. C., and Siede, W. (1995) *DNA Repair and Mutagenesis*, ASM Press, Washington, DC.
21. Friedberg, E. C., Wagner, R., and Radman, M. (2002) Specialized DNA polymerases, cellular survival, and the genesis of mutations, *Science 296*, 1627−1630.
22. Feig, D. I., Reid, T. M., and Loeb, L. A. (1994) Reactive oxygen species in tumorigenesis, *Cancer Res. 54*, 1890s-1894s.
23. Lee, D. H., O'Connor, T. R., and Pfeifer, G. P. (2002) Oxidative DNA damage induced by copper and hydrogen peroxide promotes CG→TT tandem mutations at methylated CpG dinucleotides in nucleotide excision repair-deficient cells, *Nucleic Acids Res. 30*, 3566−3573.
24. Reid, T. M., and Loeb, L. A. (1993) Tandem double CC→TT mutations are produced by reactive oxygen species, *Proc. Natl. Acad. Sci. U.S.A. 90*, 3904−3907.
25. Newcomb, T. G., Allen, K. J., Tkeshelashvili, L., and Loeb, L. A. (1999) Detection of tandem CC→TT mutations induced by oxygen radicals using mutation-specific PCR, *Mutat. Res. 427*, 21−30.
26. Gu, C., Zhang, Q., Yang, Z., Wang, Y., Zou, Y., and Wang, Y. (2006) Recognition and incision of oxidative intrastrand cross-link lesions by UvrABC nuclease, *Biochemistry 45*, 10739−10746.
27. Yang, Z., Colis, L. C., Basu, A. K., and Zou, Y. (2005) Recognition and incision of gamma-radiation-induced cross-linked guanine-thymine tandem lesion G[8,5-Me]T by UvrABC nuclease, *Chem. Res. Toxicol. 18*, 1339−1346.
28. Goodman, M. F. (2002) Error-prone repair DNA polymerases in prokaryotes and eukaryote, *Annu. Rev. Biochem. 71*, 17−50.
29. Gu, C., and Wang, Y. (2005) Thermodynamic and in-vitro replication studies of an intrastrand crosslink lesion G[8−5]C, *Biochemistry 44*, 8883−8889.
30. Johnson, R. E., Prakash, S., and Prakash, L. (1999) Efficient bypass of a thymine-thymine dimer by yeast DNA polymerase, Polη, *Science 283*, 1001−1004.
31. Masutani, C., Kusumoto, R., Yamada, A., Dohmae, N., Yokoi, M., Yuasa, M., Araki, M., Iwai, S., Takio, K., and Hanaoka, F. (1999) The XPV (xeroderma pigmentosum variant) gene encodes human DNA polymerase η, *Nature 399*, 700−704.
32. Cannistraro, V. J., and Taylor, J. S. (2004) DNA-thumb interactions and processivity of T7 DNA polymerase in comparison to yeast polymerase η, *J. Biol. Chem. 279*, 18288−18295.
33. Hong, H., and Wang, Y. (2007) Derivatization with Girard reagent T combined with LC-MS/MS for the sensitive detection of 5-formyl-2′-deoxyuridine in cellular DNA, *Anal. Chem. 79*, 322−326.
34. Hong, H., and Wang, Y. (2005) Formation of intrastrand cross-link products between cytosine and adenine from UV irradiation of d(^{Br}CA) and duplex DNA containing a 5-bromocytosine, *J. Am. Chem. Soc. 127*, 13969−13977.
35. Goodman, M. F., Creighton, S., Bloom, L. B., and Petruska, J. (1993) Biochemical basis of DNA replication fidelity, *Crit. Rev. Biochem. Mol. Biol. 28*, 83−126.
36. Creighton, S., Bloom, L. B., and Goodman, M. F. (1995) Gel fidelity assay measuring nucleotide misinsertion, exonucleolytic proofreading, and lesion bypass efficiencies, *Methods Enzymol. 262*, 232−256.
37. Stewart, J. J. P. (1989) Optimization of parameters for semiempirical methods I. Method, *J. Comput. Chem. 10*, 209−220.
38. Bellon, S., Gasparutto, D., Saint-Pierre, C., and Cadet, J. (2006) Guanine-thymine intrastrand cross-linked lesion containing oligonucleotides: from chemical synthesis to in vitro enzymatic replication, *Org. Biomol. Chem. 4*, 3831−3837.
39. Haracska, L., Washington, M. T., Prakash, S., and Prakash, L. (2001) Inefficient bypass of an abasic site by DNA polymerase η, *J. Biol. Chem. 276*, 6861−6866.
40. Haracska, L., Yu, S.-L., Johnson, R. E., Prakash, L., and Prakash, S. (2000) Efficient and accurate replication in the presence of 7,8-dihydro-8-oxoguanine by DNA polymerase η, *Nat. Genet. 25*, 458−461.
41. Kusumoto, R., Masutani, C., Iwai, S., and Hanaoka, F. (2002) Translesion synthesis by human DNA polymerase η across thymine glycol lesions, *Biochemistry 41*, 6090−6099.
42. Ito, J., and Braithwaite, D. K. (1991) Compilation and alignment of DNA polymerase sequences, *Nucleic Acids Res. 19*, 4045−4057.
43. Li, Y., Dutta, S., Doublie, S., Bdour, H. M. d., Taylor, J.-S., and Ellenberger, T. (2004) Nucleotide insertion opposite a cis-syn thymine dimer by a replicative DNA polymerase from bacteriophage T7, *Nat. Struct. Mol. Biol. 11*, 784−790.
44. Saenger, W. (1984) *Principles of Nucleic Acid Structure*, Springer-Verlag New York Inc., New York.
45. Berneburg, M., and Lehmann, A. R. (2001) Xeroderma pigmentosum and related disorders: defects in DNA repair and transcription, *Adv. Genet. 43*, 71−102.
46. Cleaver, J. E., and Kraemer, K. H. (1989) in *The Metabolic Basis of Inherited Disease* (Scriver, C., Beaudet, A. L., Sly, W. S., and Vale, D., Eds.) pp 2949−2971, McGraw-Hill, New York.
47. Reif, D. W. (1992) Ferritin as a source of iron for oxidative damage, *Free Radical Biol. Med. 12*, 417−427.
48. Calderaro, M., Martins, E. A. L., and Meneghini, R. (1993) Oxidative stress by menadione affects cellular copper and iron homeostasis, *Mol. Cell. Biochem. 126*, 17−23.
49. Carmichael, P. L., Hewer, A., Osborne, M. R., Strain, A. J., and Phillips, D. H. (1995) Detection of bulky DNA lesions in the liver of patients with Wilson's disease and primary hemochromatosis, *Mutat. Res. 326*, 235−243.
50. Cao, H., and Wang, Y. (2007) Quantification of oxidative single-base and intrastrand cross-link lesions in unmethylated and CpG-methylated DNA induced by Fenton-type reagents, *Nucleic Acids Res. 35*, 4833−4844.

BI7012195